

Structural evolution in the mechanically driven solid state amorphizing transformation of metallic alloys

This article has been downloaded from IOPscience. Please scroll down to see the full text article.

1991 J. Phys.: Condens. Matter 3 F39

(<http://iopscience.iop.org/0953-8984/3/42/004>)

View [the table of contents for this issue](#), or go to the [journal homepage](#) for more

Download details:

IP Address: 171.66.16.147

The article was downloaded on 11/05/2010 at 12:37

Please note that [terms and conditions apply](#).

Structural evolution in the mechanically driven solid state amorphizing transformation of metallic alloys

Kenji Suzuki

Institute for Materials Research, Tohoku University, Katahira 2-1-1, Aoba-ku, Sendai 980, Japan

Received 25 June 1991

Abstract. The solid state amorphizing transformations during mechanical alloying and mechanical grinding of a Ni–V binary system were observed by neutron total scattering using a spallation pulsed neutron facility. The topological mechanisms of crystal-to-amorphous solid structure transition are interpreted in terms of the transformation of octahedral structure units into tetrahedral structure units and the modification of ways of connecting tetrahedral structure units from vertex-sharing into face- and/or edge-sharing ones.

1. Introduction

Traditionally metallic amorphous alloys have been quenched from liquid or vapour phases by rapidly removing the kinetic energy of atoms moving in the energized state. As an alternative approach to conventional procedure, in this work attention has been paid to the solid state amorphizing transformation [1, 2] in which atoms in stable equilibrium crystals are mechanically excited and frozen into a metastable solid state with a topologically disordered atomic structure.

Depending on the starting materials, a mechanically driven solid state amorphizing transformation (MD-SSAT) using milling techniques can, from the thermodynamic point of view, be one of two different categories: mechanical alloying (MA) or mechanical grinding (MG). The MA process synthesizes amorphous alloys by reacting elemental crystalline powders through long distance solid state chemical diffusion, being often accompanied by a negative heat of formation. In the MG process, crystalline alloys or compounds are transformed into the amorphous solid state by destroying the periodical long-range order of atomic arrangement without long-distance movement of atoms.

Several models for the thermodynamic mechanism of MD-SSAT have been proposed: local melt-quenching [3], asymmetric solid state interdiffusion [4], excess defect accumulation [5], lowering of the melting point in supersaturated solid solutions [6], elasticity instability [7] and so on.

This paper will describe the topological rearrangement and chemical mixing of atoms during MD-SSAT of a Ni–V binary system as an example of a transition metal alloy observed by neutron total scattering. All measurements of the total neutron scattering were carried out using the HIT spectrometer installed at a spallation pulsed neutron source, KEK, Tsukuba. The MD-SSAT in both the MA and MG processes were performed using a conventional ball milling technique in an argon gas atmosphere at ambient

temperature. Detailed procedures for the experiments have been described in previous works [8, 9].

2. Topological short-range structure in the MA process

The topological structure of amorphous metals is approximately described in terms of the dense random packing of spherical atoms constructed from tetrahedral structure units exclusively [10]. In the FCC or BCC crystalline lattices, however, both tetrahedral and octahedral structure units are included in a ratio of two-to-one. This implies that octahedral structure units have to be transformed into tetrahedral structure units during the MA process if amorphous alloys are directly synthesized from FCC or BCC lattices without formation of intermediate crystalline phases.

Fukunaga *et al* [11] and Suzuki [12] have observed the topological structure change during the MA process of $4\text{Ni}(\text{FCC}) + 6\text{V}(\text{BCC}) \rightarrow \text{V}_4\text{Ni}_6(\text{amorphous})$ as a function of milling time by total neutron scattering. The angular differential cross section $(d\sigma_c/d\Omega)_{\text{total}}$ for a Ni-V binary alloy measured by total neutron scattering is related to the Faber-Ziman [13] total neutron structure factor $S(Q)$:

$$(d\sigma_c/d\Omega)_{\text{total}} = N\langle b \rangle^2 S(Q) + N(\langle b^2 \rangle - \langle b \rangle^2) \quad (1)$$

where $\langle b \rangle = c_{\text{Ni}}b_{\text{Ni}} + c_{\text{V}}b_{\text{V}}$, $\langle b^2 \rangle = c_{\text{Ni}}b_{\text{Ni}}^2 + c_{\text{V}}b_{\text{V}}^2$, $\langle b \rangle^2 = (c_{\text{Ni}}b_{\text{Ni}} + c_{\text{V}}b_{\text{V}})^2$, c_i and b_i are the concentration fraction and coherent neutron scattering length of an i -species atom, N is the number of chemical formula units involved in the alloy sample and $Q = 4\pi \sin \theta / \lambda$. Results in figure 1 are shown in terms of the Faber-Ziman formalism.

The Faber-Ziman total neutron structure factors $S(Q)$ for a Ni-V alloy are expressed as a weighted sum of three partial structure factors $S_{\text{NiNi}}(Q)$, $S_{\text{NiV}}(Q)$ and $S_{\text{VV}}(Q)$ associated with Ni-Ni, Ni-V and V-V pair correlations:

$$S(Q) = w_{\text{NiNi}}S_{\text{NiNi}}(Q) + 2w_{\text{NiV}}S_{\text{NiV}}(Q) + w_{\text{VV}}S_{\text{VV}}(Q) \quad (2)$$

where $w_{ij} = c_i c_j b_i b_j / \langle b \rangle^2$ is the weighting factor for the i - j pair correlation. The $S(Q)$ of Ni-V alloys can be approximated to the Ni-Ni partial structure factors $S_{\text{NiNi}}(Q)$ except in the extremely low Ni-content region, because the coherent neutron scattering length of a V nucleus ($b_{\text{V}} = -0.0382 \times 10^{-12}$ cm) is negligibly small compared with that of a Ni nucleus ($b_{\text{Ni}} = 1.03 \times 10^{-12}$ cm).

Bragg reflection peaks observed for a Ni(FCC) crystal, as shown in figure 1, are already widened even before milling due to a broad resolution of the HIT spectrometer, which is designed for the measurement of liquid and amorphous structure factors. Thus, we do not discuss the initial stage, corresponding to the break of long-range order in the Ni(FCC) lattice by mechanical milling.

The prepeak located around $Q = 1.9 \text{ \AA}^{-1}$ begins to appear after 100 h of milling time. With a further increase of milling time, the prepeak becomes very obvious and the negative height is contributed to this in the low- Q range below about 1.5 \AA^{-1} . Such behaviour of the prepeak has been found commonly in the $S_{\text{NiNi}}(Q)$ of Ni-early transition metal amorphous alloys prepared by sputter deposition and melt quenching [14]. However, we cannot exclude the possibility of a negative height being caused by the disordered medium-range ($\sim 10 \text{ \AA}$) correlation between Ni and V atoms existing in the non-uniform amorphous solid state.

The neutron total structure factor of MA amorphous alloys often shows significant intensity in the small-angle scattering region corresponding to $Q < 0.3 \text{ \AA}^{-1}$ [9]. Such a

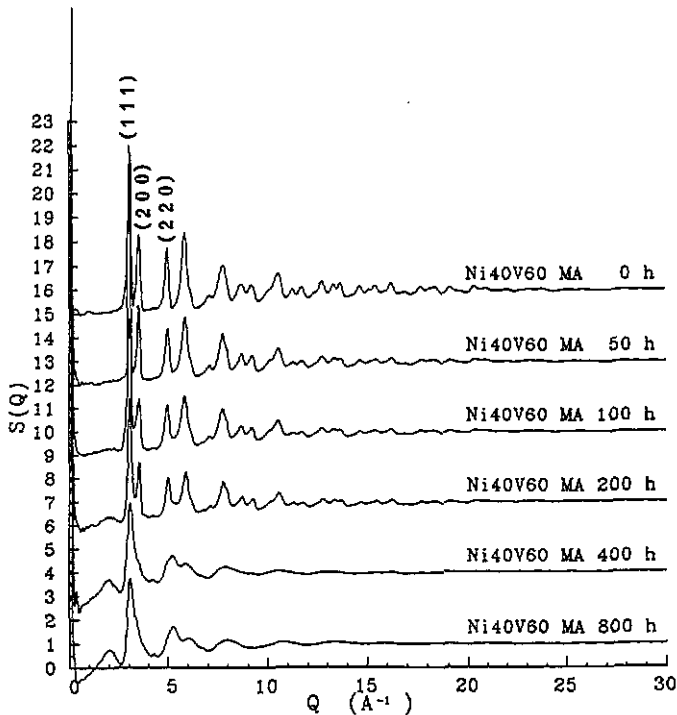


Figure 1. Neutron total structure factors $S(Q)$ for the MA process of $4\text{Ni}(\text{FCC}) + 6\text{V}(\text{BCC}) \rightarrow \text{Ni}_4\text{V}_6(\text{amorphous})$ as a function of milling time.

small angle scattering intensity can be also observed during the MA process of Ni–V binary system. This means that Ni–V amorphous alloys prepared by the MA process are not completely uniform in the medium/long-range scale ($\sim 100 \text{ \AA}$) structure.

When milling time is greater than 400 h, the (200) Bragg reflection peak is practically lost and vibrations in high- Q region disappear. The rapid reduction in the (200) peak height suggests that octahedral structure units in the Ni(FCC) lattice are almost totally destroyed during the MA process.

The phenomenon suggested above is clearly demonstrated in the neutron radial distribution functions RDF defined as the Fourier transform of the Faber–Ziman neutron total structure factors $S(Q)$ truncated at $Q_{\text{max}} = 30 \text{ \AA}^{-1}$ (figure 1) without using any artificial modification functions. As shown in figure 2, the second peak located around $r = 3.5 \text{ \AA}$ and the fifth peak around $r = 5.6 \text{ \AA}$ are lost drastically with increasing milling time, while the other peaks are only broadened. Figure 3 is an illustration of the FCC lattice, in which the second and fifth neighbouring atoms surrounding a central atom just occupy the key sites so constructing octahedral structure units. Therefore, the characteristic behaviour of RDF observed in figure 2 certainly suggests that the topological mechanism of MD-SSAT starting from the FCC crystal is based on the transition of octahedral structure units into tetrahedral structure units.

3. Topological short-range structure in the MG process

Figure 4 shows changes in the Faber–Ziman neutron total structure factors $S(Q)$ as a function of milling time for the MG process of the Ni_4V_6 intermetallic compound starting

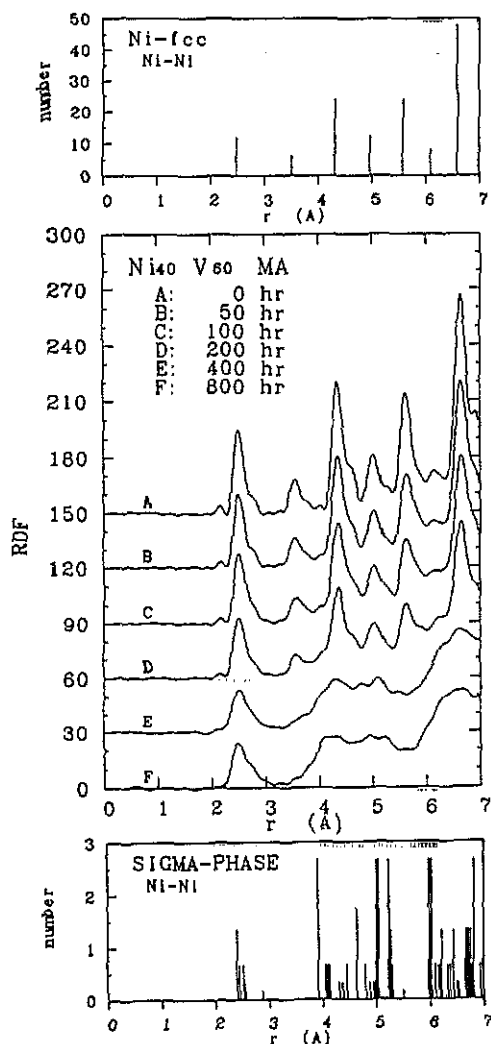


Figure 2. Neutron RDFs for the MA process of $4\text{Ni}(\text{fcc}) + 6\text{V}(\text{BCC}) \rightarrow \text{Ni}_4\text{V}_6(\text{amorphous})$ as a function of milling time.

from the crystalline state (σ phase, space group; $P4_2/mnm$). The MG process provides broadening of Bragg reflection peaks, with less ripples in the high Q region, $Q > 5 \text{ \AA}^{-1}$, and drastic changing in peak profiles located in the low Q region, $Q < 4 \text{ \AA}^{-1}$. In contrast to the MA process of a mixture of Ni and V powders, no small-angle scattering intensities appear in $S(Q)$ during the Ni_4V_6 compound MG process.

The first sharp diffraction peak corresponding to the (101) Bragg reflection peak is abruptly and severely diminished. However, the (220) peak just remains, forming a so-called prepeak as often observed in the neutron $S(Q)$ of Ni-early transition metal amorphous alloys [14]. The subpeaks located on both sides of the (411) main peak broaden to form a single halo by overlapping with the main peak. The peaks in $S(Q)$ are never equally modified during the MG process, but only specified peaks follow selectively dramatic evolutions.

The neutron total radial distribution functions RDF of Ni_4V_6 alloys are defined by Fourier transforming the $S(Q)$ truncated at $Q_{\text{max}} = 30 \text{ \AA}^{-1}$. Results are shown in figure

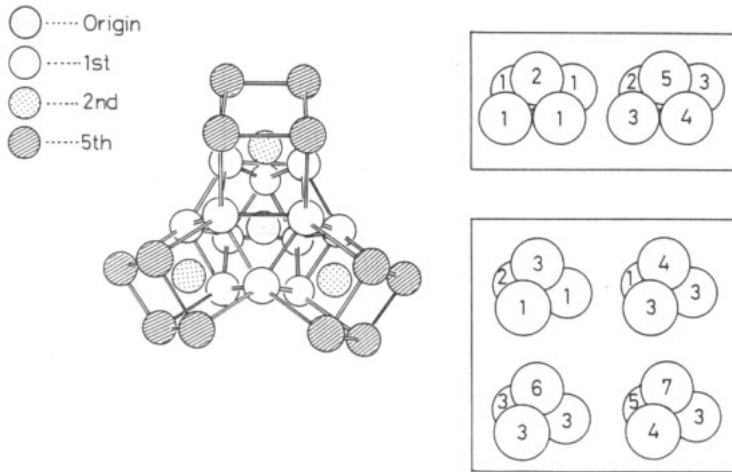


Figure 3. Atomic arrangement surrounding a central atom in a FCC lattice.

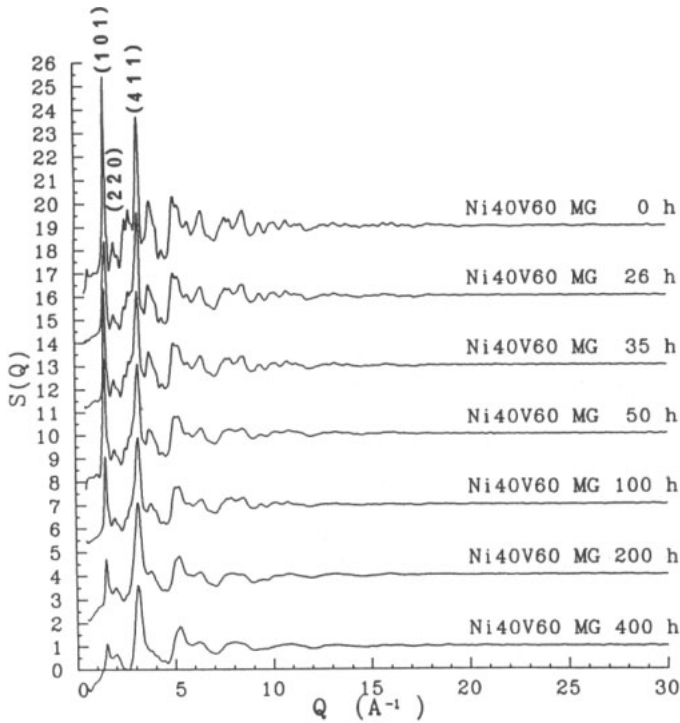


Figure 4. Neutron total structure factors $S(Q)$ for the MG process of Ni_4V_6 (crystalline σ phase) \rightarrow Ni_4V_6 (amorphous) as a function of milling time.

5. The first peak, located at around $r = 2.5 \text{ \AA}$, represents the first nearest neighbours in Ni–Ni correlations, of which distance and coordination number are little changed between the beginning and end of the MG process. The second peak appearing around

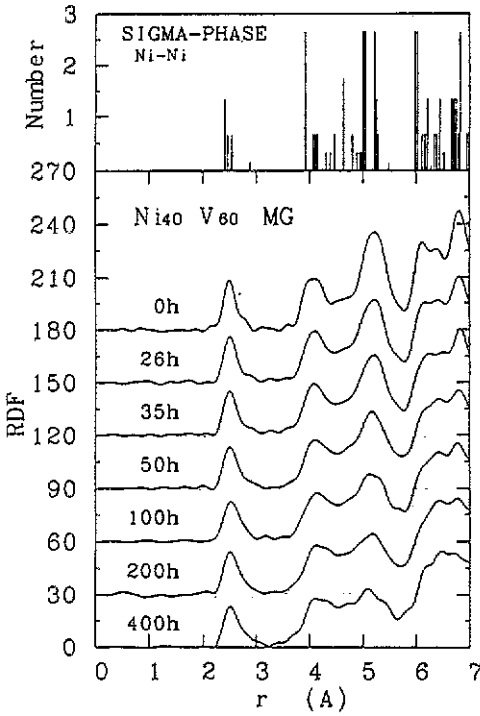


Figure 5. Neutron total RDFs for the MG process of Ni_4V_6 (crystalline σ phase) \rightarrow Ni_4V_6 (amorphous) as a function of milling time.

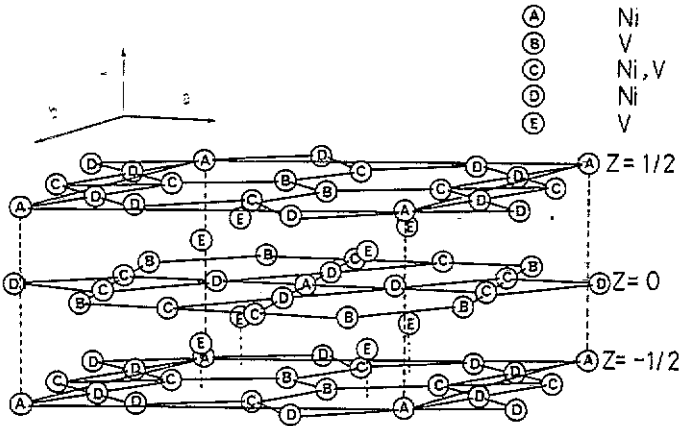


Figure 6. Atomic arrangement in a unit cell of crystalline σ phase.

$r = 4 \text{ \AA}$ never shows significant variations in its profile. The third peak located slightly above $r = 5 \text{ \AA}$ is dramatically widened and lowered with progressing MG process. The intermediate region between the second peak and the third one rises gradually with increasing milling time.

The atomic arrangement in a unit cell constructing the crystalline σ phase is illustrated in figure 6. Atoms in the unit cell occupy the five different kinds of topological sites. A and D sites in figure 6 are only occupied by Ni atoms, while B and E sites are only

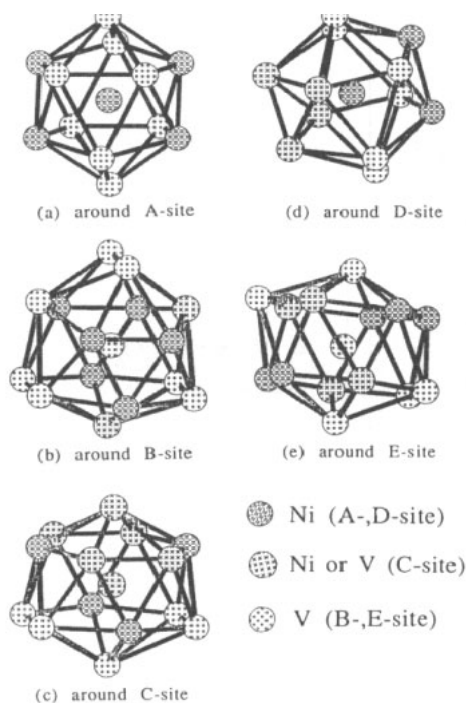


Figure 7. Coordination polyhedra existing in a crystalline σ phase.

occupied by V atoms. The C site is occupied by Ni or V atoms according to the Ni-to-V atom ratio in σ phase.

Atomic environments surrounding the five different sites in the σ phase are represented in terms of the coordination polyhedra, which are illustrated in figure 7. Both A and D sites are the centres of 12-coordinated icosahedra including pentagonal configurations, which are characteristically found in quasicrystalline and amorphous metals. As in Frank-Kasper phases, all the polyhedra shown in figure 7 are constructed from tetrahedral structure units. There are three possible ways of connecting tetrahedral structure units to each other in these coordination polyhedra: face sharing, edge sharing or vertex sharing, as shown in figure 8.

All the Ni-Ni correlations existing in the coordination polyhedra can be classified into three groups according to the three kinds of sharing in tetrahedral structure units. As shown in figure 8, however, there is an extreme case where it is difficult to distinguish between edge sharing and face sharing [15]. Therefore, the classification of Ni-Ni distances belonging to inter-tetrahedral structure units into three groups cannot be unique. If the Ni-Ni nearest-neighbour distance in an intra-tetrahedral structure unit is about 2.5 Å, the Ni-Ni distances in inter-tetrahedral structure units are about 5 Å for vertex sharing and 4 Å for face sharing, respectively.

As some of the tetrahedral structure units existing in the coordination polyhedra, shown in figure 7, are distorted, and the connecting angles for vertex sharing or edge sharing of two tetrahedral structure units vary, the Ni-Ni distances in inter-tetrahedral structure units are broadly spread around $r = 4$ and 5 Å, respectively. The Ni-Ni distances existing in the intermediate region between $r = 4$ and 5 Å come partly from the edge-sharing of two-tetrahedral structure units. The three way distribution of Ni-Ni

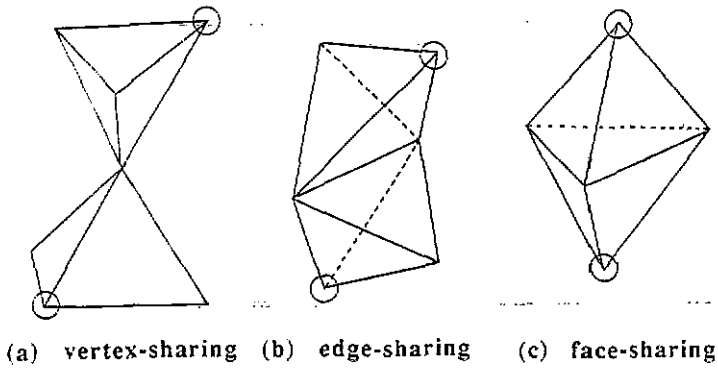


Figure 8. Three possible ways of connecting tetrahedral structure units.

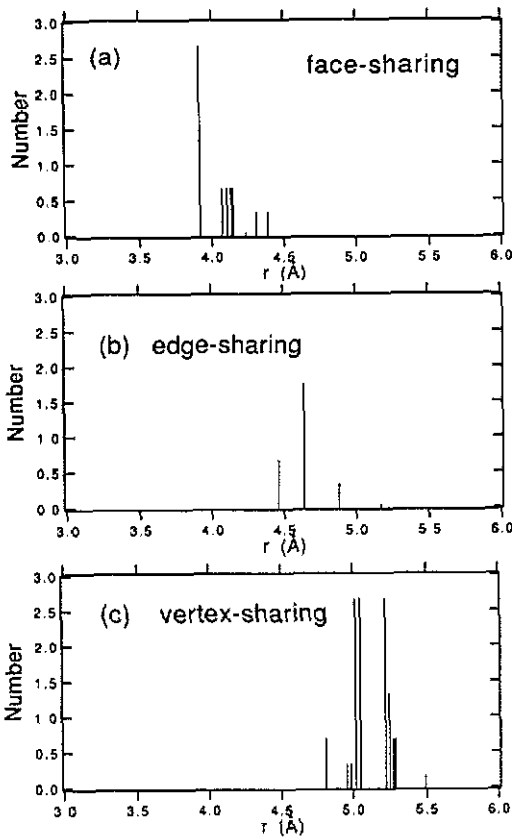


Figure 9. The classification of Ni-Ni distances found in coordination polyhedra in Ni_4V_6 crystalline σ phase into three possible ways of connecting tetrahedral structure units.

distances for connecting tetrahedral structure units existing in σ phase is shown in figure 9.

Based on the result of figure 9, we can conclude that the second peak around $r = 4 \text{ \AA}$ in RDF corresponds to the face-sharing Ni-Ni correlation in inter-tetrahedral structure units, which almost remains, without significant changes, during MG process. On the

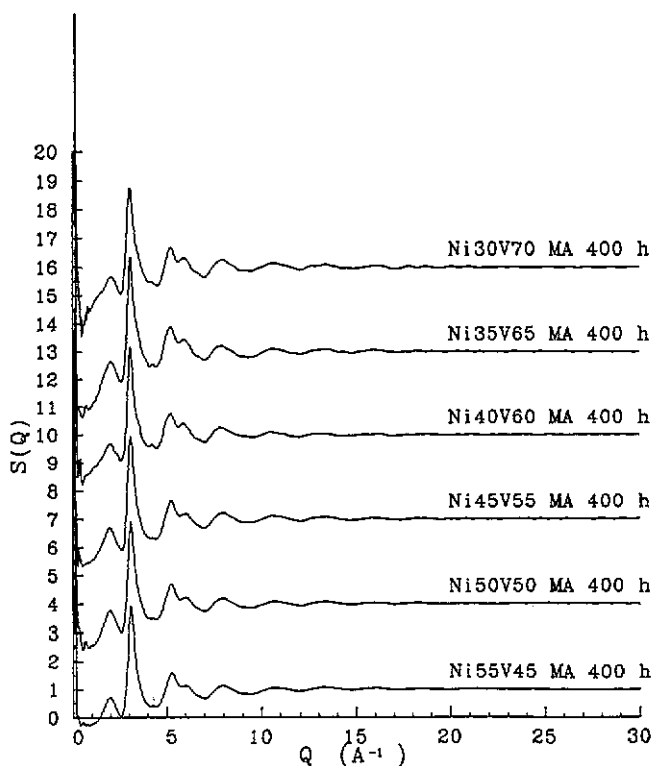


Figure 10. Neutron total structure factors $S(Q)$ of Ni-V amorphous alloys prepared by the MA process as a function of V content.

other hand, the third peak around $r = 5 \text{ \AA}$ in the RDF corresponds to the vertex-sharing Ni-Ni correlation in inter-tetrahedral structure units, which is drastically destroyed with the progress of milling. This implies that the conversion from vertex sharing to face sharing between tetrahedral structure units preferentially happens along with the distortion of the tetrahedral structure unit during the MG process of the Ni_4V_6 (σ phase) crystalline intermetallic compound.

4. Chemical short-range order in MA amorphous alloys

The ball milling technique can provide Ni-V amorphous alloys over a wide chemical composition range from 45 to 70 at.% V [16], which includes the whole region of crystalline σ phase in its equilibrium phase diagram. Figure 10 shows, as a function of V content, the neutron total structure factors $S(Q)$, which are almost the same as the Ni-Ni partial structure factors $S_{\text{NiNi}}(Q)$, of Ni-V amorphous alloys obtained after 400 h of the MA process. The overall behaviour of $S_{\text{NiNi}}(Q)$ is found to be almost the same over the entire chemical composition range.

The neutron radial distribution functions RDF for the Ni-Ni correlation in Ni-V amorphous alloys, defined as the Fourier transform of $S(Q)$ truncated at $Q_{\text{max}} = 23 \text{ \AA}^{-1}$,

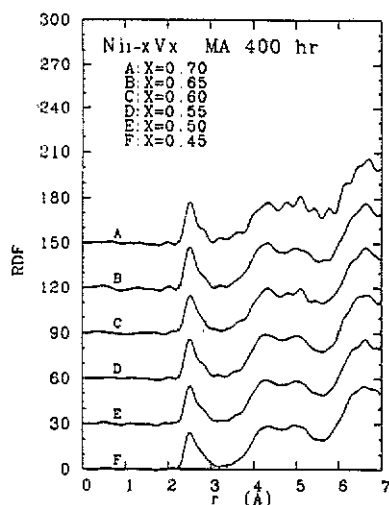


Figure 11. Neutron total RDFs of Ni-V amorphous alloys prepared by the MA process as a function of V content.

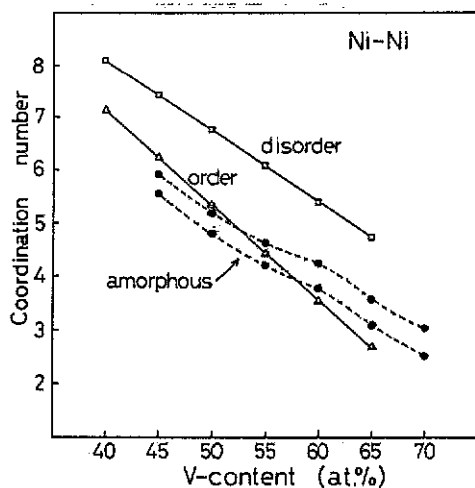


Figure 12. Coordination numbers of Ni atoms around a Ni atom in a MA amorphous alloy, ordered σ phase and disordered σ phase of a Ni-V binary system as a function of V content.

are shown as a function of V content in figure 11. The RDF are also very similar to each other. The behaviour mentioned above suggests that the Ni-Ni correlation is rigidly preserved with little change over the whole range of chemical composition in Ni-V amorphous alloys.

In order to evaluate the chemical short-range order persisting in Ni-V amorphous alloys prepared by the MA process, we obtain the coordination numbers of Ni atoms around a Ni atom by calculating the area under the first peak of the RDF. Results are shown in figure 12 in which the shaded area corresponds to the range of contributions from the Ni-V correlation to the first peak area in the RDF.

The crystalline σ phase (space group; $P4_2/mnm$) has a definite degree of the chemical order among five different atomic sites in its unit cell, as shown in figure 6. We suppose a chemically disordered σ phase [16] in which both the Ni and V atoms are randomly distributed on all sites of the unit cell. The coordination numbers of Ni-Ni correlations in both the chemically ordered and disordered Ni-V σ -phase alloys are plotted as a function of V content in figure 12.

Figure 12 shows that the coordination number of Ni-Ni correlations in Ni-V amorphous alloys prepared by the MA process follows those in the chemically ordered σ phase quite closely. This means that the MA process, starting from elemental Ni and V metal, provides the atomic-scale mixing of metallic elements to form homogeneous Ni-V amorphous alloys, of which chemical short-range structures are rather similar to those of their crystalline counterparts of ordered σ -phase alloys.

It is noteworthy that the range of chemical composition over which Ni-V amorphous alloys can be formed by the MA process is apparently wider than that of the crystalline σ phase found in the equilibrium phase diagram of the Ni-V binary system and is extended to the side of lower V content. However, as shown in figure 13, the position of the prepeak in the neutron $S(Q)$ of Ni-V amorphous alloys is sharply decreased within the range of single- σ phase with decreasing V content, but remains nearly constant in

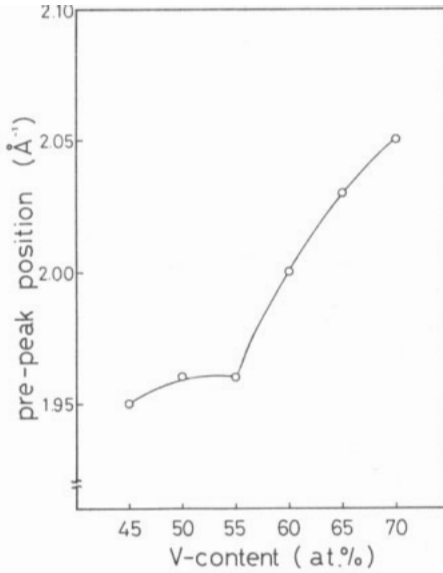


Figure 13. Position of the prepeak in the neutron $S(Q)$ of Ni-V amorphous alloys prepared by the MA process as a function of V content.

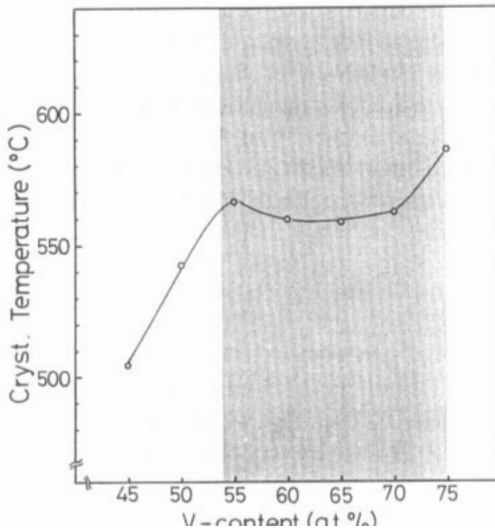


Figure 14. Crystallization temperature of Ni-V amorphous alloys prepared by the MA process as a function of V content.

the range of V content less than 55 at. %V outside the single- σ phase range, which corresponds to the two-phase mixture of the σ phase and the Ni_2V phase. Figure 14 also shows that the crystallization temperature of Ni-V amorphous alloys is nearly constant,

around 570 °C within the single- σ phase range. These observations suggest again the strong conservation of chemical short-range order of the crystalline σ phase even in Ni-V amorphous alloys prepared by the MA process.

5. Concluding remarks

The structural evolution in the solid state amorphizing transformation was observed for both the MA and the MG of a Ni-V binary system by neutron total scattering using a spallation pulsed neutron facility. The topological mechanism of the crystal-to-amorphous solid structure transition can be interpreted in terms of the mutation of an octahedral structure unit into a tetrahedral structure unit, and the reconnecting of tetrahedral structure units by vertex sharing to face and/or edge sharing.

The Ni-V binary system is a compound-forming system accompanied by a negative heat of formation. Although the Cu-Ta binary system is an immiscible system, having a positive heat of formation in the equilibrium state, it is expected that the topological mechanism for the solid state formation of Cu-Ta amorphous alloys by mechanical alloying [17] is essentially similar to that observed for the Ni-V binary system.

The atomic-scale mixing during mechanical alloying of Ni and Ti metals has been verified directly by observing the Bhatia-Thornton [18] partial structure factor $S_{CC}(Q)$ for the concentration-concentration correlation in a Ni_{24.3}Ti_{75.7} neutron zero-scattering alloy [19].

The broadening of Bragg reflection peaks in the crystalline state is rapidly saturated at an early stage of mechanical milling. The breaking of the long-range order in the crystalline state by accumulating defects is not directly transferred to the amorphizing transformation, in which topological rearrangements in the short- and medium-range order have to take place as described in this paper. Careful observations of $S(Q)$ in the range of small- and wide-angle scattering overlap should be helpful to the investigation of the total mechanism of the structural evolution from crystal to amorphous solid. The relationship between the topological mechanism and the thermodynamic mechanism of a mechanically driven solid state amorphizing transformation is also of interest and we hope to investigate this next.

Acknowledgments

The author would like to thank T Fukunaga, Y Homma and M Misawa for their great contributions during the investigation. This work was supported by Grant-in-Aid for Developmental Research (B) 03555139 the Ministry of Education, Science and Culture, Japan.

References

- [1] Schwarz R B and Johnson W L (ed) 1988 *Proc. Conf. on Solid State Amorphizing Transformations* (Amsterdam: North-Holland); *J. Less-Common Met.* **140**
- [2] Endo H (ed) 1990 *Proc. 7th Int. Conf. on Liquid and Amorphous Metals* (Amsterdam: North-Holland); *J. Non-Cryst. Solids* **117/118**
- [3] Yermakov A Y, Yurchikov Y Y and Barinov V A 1981 *Phys. Met. Metallogr.* **52** 50
- [4] Schwarz R B, Petrich R R and Saw C K 1985 *J. Non-Cryst. Solids* **76** 281

- [5] Koch C C, Cavin O B, McKamey C G and Scarborough J O 1983 *Appl. Phys. Lett.* **43** 1017
- [6] Fecht H J, Han G, Fu Z and Johnson W L 1990 *J. Appl. Phys.* **67** 1744
- [7] Johnson W L 1986 *Prog. Mater. Sci.* **30** 81
- [8] Suzuki K 1987 *Method of Experimental Physics—Neutron Scattering* vol 23B, ed D L Price and K Sköld (New York: Academic) p 243
- [9] Suzuki K 1989 *J. Non-Cryst. Solids* **112** 23
- [10] Finney J L and Wallace J 1981 *J. Non-Cryst. Solids* **43** 165
- [11] Fukunaga T, Homma Y, Misawa M and Suzuki K 1990 *J. Non-Cryst. Solids* **117/118** 721
- [12] Suzuki K 1990 *J. Non-Cryst. Solids* **117/118** 1
- [13] Faber T E and Ziman J M 1965 *Philos. Mag.* **11** 153
- [14] Fukunaga T, Urai S, Watanabe N and Suzuki K 1988 *J. Phys. F: Metal Phys.* **16** 99
- [15] Homma Y, Fukunaga T, Misawa M and Suzuki K 1991 *Proc. Int. Symp. of Mechanical Alloying (Kyoto, 1991)* ed P H Shingu (Kyoto: The Japan Society of Powder and Powder Metallurgy) at press
- [16] Fukunaga T, Homma Y, Misawa M and Suzuki K 1991 *Mat. Sci. and Eng. A* **134** 987
- [17] Lee C H, Fukunaga T and Mizutani U 1991 *Mat. Sci. and Eng. A* **134** 1334
- [18] Bhatia A B and Thornton D E 1970 *Phys. Rev. B* **2** 3004
- [19] Fukunaga T, Misawa M, Suzuki K and Mizutani U 1991 *Proc. Int. Symp. of Mechanical Alloying (Kyoto, 1991)* ed P H Shingu (Kyoto: The Japan Society of Powder and Powder Metallurgy) at press